# Rationalization of Nanowire Synthesis Using Low-Melting Point Metals

**Hari Chandrasekaran,[†] Gamini U. Sumanasekara,[‡] and Mahendra K. Sunkara*[,†]**

*Department of Chemical Engineering, Department of Physics, University of Louisville, Louisville, Kentucky 40292*

*Received: June 26, 2006; In Final Form: July 25, 2006*

In this paper, we provide a theoretical basis using thermodynamic stability analysis for explaining the spontaneous nucleation and growth of a high density of 1-D structures of a variety of materials from low-melting metals such as Ga, In, or Sn. The thermodynamic stability analysis provides a theoretical estimate of the extent of supersaturation of solute species in molten metal solvent. Using the extent of maximum supersaturation, the size and density of critical nucleus were estimated and compared with experimental results using nucleation and growth of Ge nanowires using Ga droplets. The consistency of the proposed model is validated with the size and density of the resulting nanowires as a function of the synthesis temperature and droplet size. Both the experimental evidence and the theoretical model predictions point that the diameters of the resulting nanowires decrease with the lowering of synthesis temperatures and that the nucleation density decreases with the size of metal droplet diameter and increasing synthesis temperature.



## Introduction

The vapor−liquid−solid (VLS) method is a well-accepted technique for growing 1-D structures with diameters ranging from micrometers (whiskers) to nanometers (nanowires). The main aspect of this method is that the diameter of the precipitating 1-D crystal is controlled by limiting the size of the catalytic metal cluster which is used as the template. This well-established concept, from the early 1960s, has become a technology of interest for many researchers.[1]

Earlier, we showed that Si nanowire growth using low-melting metal droplets is not limited by the cluster size and occurs at a high density from a single droplet.[2] Later, this concept has been used for demonstrating the synthesis of several materials systems such as Si, Bi, amorphous $SiO_2$, and $Si_xN_yH$ nanowires.[3] In particular, the direct synthesis of nanowires of compounds of low-melting metals such as Group III-nitrides, sulfides, oxides, and so forth[4] under metal-rich conditions fall under this concept as well. All these experimental observations point toward a concept different from the traditional concept of catalytic metal cluster enabled 1-D growth. The main difference is that high density of nucleation occurs out of one large-sized droplet and the nucleation defines the size of the resulting nanowires. In addition, this method avoids foreign metal contamination for many systems and produces a high density of nanowires thus generating an increased interest in this method.[5] However, it is important to understand the underlying concept of nucleation to rationalize this concept and to make it a useful technique for controlled synthesis of nanowires.

Most vapor−liquid−solid processes including the present one with low-melting metals are typically carried out under isothermal conditions. In these cases, the concentration supersaturation at which the nucleation occurs is poorly defined for liquid−solid-phase transitions. Typically, the constitutional undercooling experiments have been employed to understand the solute precipitation out of binary systems.[6] In these experiments, it is easy to estimate the extent of supersaturation as the difference in the solubility limit at the two known temperatures. In the absence of such experimental data for nanowire synthesis, we investigated the possibility of using thermodynamic stability analysis to determine the concentration supersaturation at which the supersaturated melts instantaneously separate into solid and liquid phases. The proposed model is then used to predict the critical nucleus diameter and resulting nucleation density of nanowires. These theoretical predictions are further validated using the experimental studies on Ge nanowire synthesis using Ga and other low-melting metal droplets. The thermodynamic model proposed here deals mainly with binary systems (solute−solvent) and cannot be directly applied to systems that consist of more than one solute species.

Recently, the functionalized bismuth nanocrystals have been used to seed the growth of Ge nanowires without undergoing a nucleation step in a supercritical fluid environment.[7] Here, we show for the first time the bulk nucleation and growth of Ge nanowires at high densities from individual, large droplets of Ga and other low-melting metals. The difficulty in the synthesis of Ge nanowires as opposed to Si nanowires using Ga melt arises because of the quantitative differences between the Ge−Ga and Si−Ga binary phase diagrams shown in Figure 1. Ge has a significantly lower melting point (∼937 °C) as compared to Si (1410 °C) causing the change in equilibrium solubility with temperature, $\delta X^l_2/\delta T$, and the eutectic composition to be $\sim 10^4$ times greater in Ge/Ga system as compared to Si/Ga system.[6] Most importantly, the solubility of Ge in Ga although relatively low is 5 orders of magnitude higher than that of Si in Ga at its eutectic temperature.[6] Unlike Si, Ge partially wets gallium at 300 °C[8] in the absence of any gas-phase chemistry effects. Thus, the Ge nucleation and growth using Ga melts is interesting for studying the conditions that favor the growth of nuclei in 1-D and not in either 2-D or 3-D. Also, the synthesis of Ge nanowires is of interest for both biomedical and electronic applications as Ge exhibits an indirect band gap at 0.66 eV and

* Author to whom correspondence should be addressed. E-mail: mahendra@louisville.edu.
[†] Department of Chemical Engineering.
[‡] Department of Physics.

10.1021/jp0639750 CCC: $33.50 
Published on Web 08/30/2006

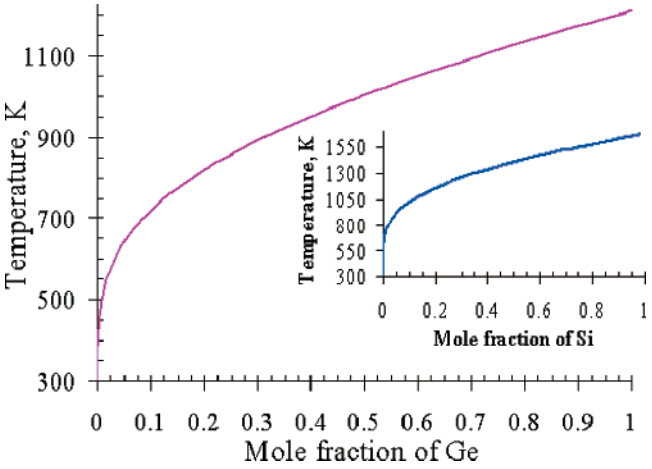


**Figure 1.** Binary phase diagram of Ge−Ga calculated using regular solution model,[5] showing the formation of a eutectic alloy with Ge composition of $10^{-5}$ at. % and at 302 K. The inset shows the Si−Ga binary system with a eutectic alloy at $10^{-10}$ at. %, at ~302 K.

a direct band gap at 0.8 eV.[9] The synthesis of sub-10-nm-sized Ge nanowires with monosize distribution is also of interest for understanding the size-dependent electronic and phonon confinement effects.

## Experimental Details

Two types of nanowire synthesis experiments were conducted: solid−liquid−solid (SLS) type growth experiments and vapor−liquid−solid (VLS) type growth experiments. Typically, the SLS growth experiments were conducted by spreading a thin film of molten metal on a clean ⟨100⟩ undoped, *n*-type Ge single-crystal wafer and exposing it to microwave plasma containing $H_2$ diluted in $N_2$ ($H_2$:N2 10:100 ratio). The required chlorine is provided through ~2 mg of NaCl crystals (finely powdered using mortar−pestle) placed around the substrate. The reactor pressure and MW power were varied between 15 and 30 Torr and between 300 and 600 W, respectively. The VLS growth experiments were conducted by spreading a thin film of molten metal on ultrasonically cleaned (in acetone) fused silica quartz substrate. A powder mixture containing Ge and NaCl (Ge:NaCl 100:2 ratio) was placed around the quartz substrate to provide the chemical vapor transport of Ge using chlorine. The reactor pressure and MW power were varied between 15 and 30 Torr and between 500 and 800 W, respectively.

The substrate temperature was calibrated using melting of different metals, In (mp = 156.6 °C), Sn (mp = 232 °C), Bi (mp = 271.3 °C), Zn (mp = 420 °C), and Al (mp = 660 °C). The resulting nanowires were characterized using Ziess field emission scanning electron microscope (FESEM), JEOL 2010 HRTEM for morphology, structure, and growth direction. Raman scattering measurements on an ensemble of Ge nanowires were performed at room temperature using a Renishaw inVia micro-Raman system consisting of a cooled CCD detector and a confocal microscope with a 50× objective lens. The spot size at the sample was approximately 1 $\mu$m. The excitation source was a 17 mW (max) HeNe laser with 632.8-nm radiation. Measurements at various laser excitation powers were performed using various combinations of neutral density filters.

## Results and Discussion

The synthesis experiments were performed in a microwave (MW) plasma reactor (ASTeX 5010). Two configurations were used for the supply of Ge: (a) the placement of Ga droplets on Ge substrate allowed for direct dissolution of Ge through solid−liquid interface and (b) the chemical vapor transport of Ge through vapor phase using chlorine and hydrogen onto low-melting metal droplets placed on amorphous quartz and polycrystalline diamond substrates for Ge dissolution through vapor−liquid interface; see Figure 2. NaCl powder was used for providing the chlorine in the gas phase.

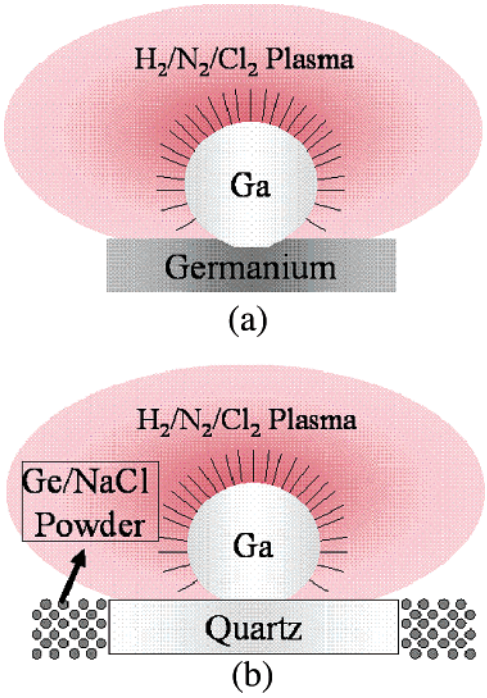


**Figure 2.** Schematics illustrating the two types of growth experiments performed using $H_2/N_2$ plasma in the MW reactor: (a) SLS mode and (b) VLS mode.

Figure 3 shows the results obtained with chemical vapor transport experiments performed at a pressure of 30 Torr and 400 W MW power, using 10 sccm of $H_2$ diluted in 100 sccm of $N_2$. The SEM micrographs in Figure 3b clearly show high densities of Ge nanowires with monosize distribution resulting from micrometer-sized molten Ga droplets at substrate temperatures between 300 and 450 °C. The near-spherical shape of the Ga droplet (not shown) suggests that the interfacial energy between the substrate and the solute is quite high. Quantitative analysis using SEM images suggests that the nanowire diameter distribution is monosize within the SEM resolution (about 2 nm), as shown in Figure 4a. High-resolution transmission electron micrograph (HR-TEM) of a 7-nm-diameter Ge nanowire does not show the presence of any oxide sheath with a growth direction of [211]; see Figure 4b.

The overall results with Ge and Si nanowire synthesis using several low-melting metals such as In and Sn yielded similar results to that using Ga droplets, that is, high densities of nanowires resulted from micrometer-sized droplets. In all cases, the observed monosize distributions of diameters and lengths of Ge and Si nanowires suggest spontaneous nucleation. To explain such behavior, we explore the possibility that the binary systems involving low-melting metal melts as solvents could exhibit miscibility gap with solutes under the presence of atomic hydrogen and chlorine in the gas phase.

The solutal segregation from the binary solution through nucleation at the point of the solubility limit or the spinodal limit could occur instantaneously by decomposition into pure solid and binary liquid phases. The nucleated crystals could only grow vertically outward from the solvent if the lateral growth

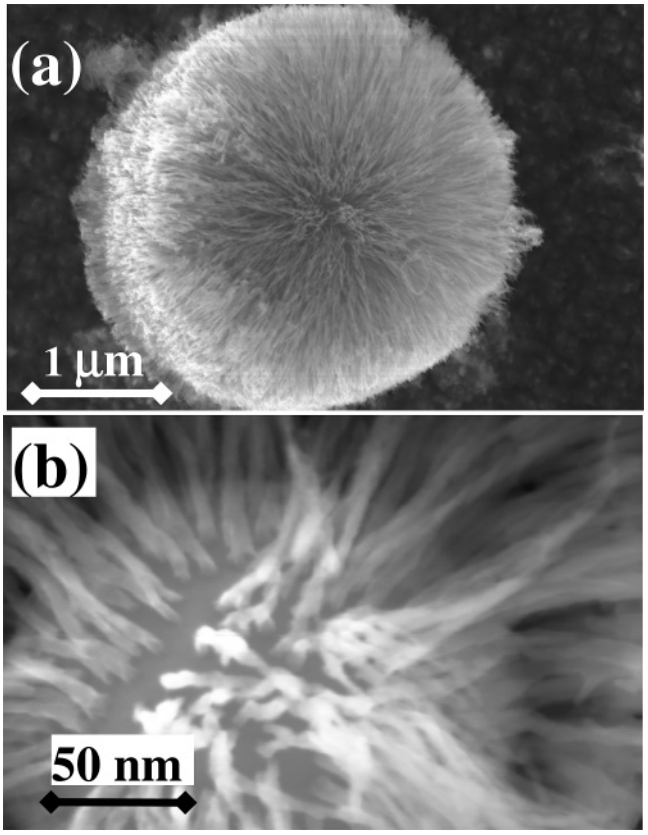


**Figure 3.** The SEM micrographs showing Ge nanowires grown in an SLS mode at 500 W microwave power and at 30 Torr pressure for 1 h using 10 sccm of $H_2$ diluted in 100 sccm $N_2$: (a) SEM image showing a high density of Ge nanowires of approximately the same length and diameter growing selectively out of a 3-$\mu$m-sized Ga droplet; (b) Ge nanowires of 10-nm diameter growing from a 400-nm-sized Ga droplet; (c) low-magnification micrograph showing Ge nanowire growth from Ga droplets on Ge substrate over a large area.



is restricted with high interfacial tension between the solute and the solvent. Thus, the initial nucleus size determines the diameter of the resulting nanowires (not the nucleation density). So, the overall nucleation model is proposed as follows. The binary solution involving the low-melting metal and the solute, at any given temperature, exhibits a solubility limit beyond which the solution becomes thermodynamically unstable. The supersaturation setup by the solute concentrations at the solubility limit and the liquidus line determines the size of the crystal nucleus or the eventual diameter of the nanowire. Further growth of the nanowire occurs through basal attachment of the precipitating solute onto the preexisting nucleus at the nucleus−liquid interface. We believe that this mechanism should be applicable for all circumstances irrespective of the gas-phase activation method used such as thermal or plasma.[4,5] This hypothesis is illustrated further with the Gibbs' stability criterion.

For a binary system, the equilibrium between the solution and the solid exists when the free energy of mixing is the lowest for any given temperature. This gives rise to the liquidus line in the binary phase diagram. Mathematically,

$$\left(\frac{\partial G_l}{\partial X_{\mathrm{Ge}}}\right)_{T,P} = 0 \qquad (1)$$

The concentration that satisfies the above equation is the equilibrium solubility of the solute at a given temperature. Metastable regions in the phase diagram are known to exist

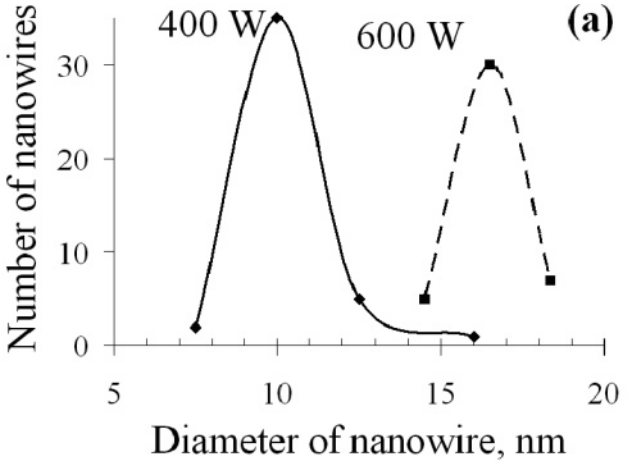


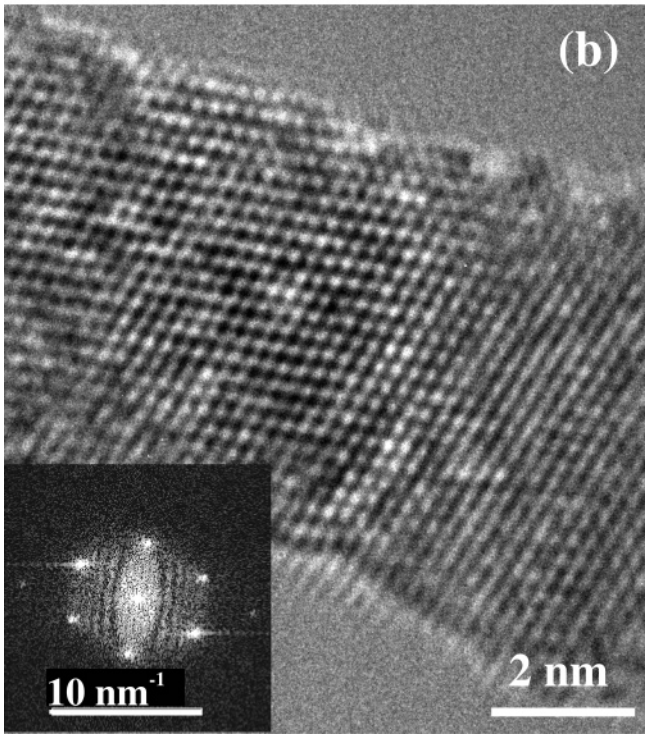


**Figure 4.** (a) Histogram showing the diameter distribution of nanowires resulting from an SLS experiment conducted at 30 Torr pressure and 500 W and (b) an HR-TEM micrograph showing a 5-nm-diameter Ge nanowire with a growth direction of ⟨112⟩ devoid of any oxide sheath.

where the solution is supersaturated with the solute species and does not phase segregate.[10] Continuous nucleation and growth from such metastable melts is quite possible, as predicted by classical nucleation theory. Alternatively, it is also possible to destabilize the supersaturated melt such that the phase segregation occurs spontaneously. The critical limit (neutral stability) of the solution beyond which the solution spontaneously decomposes into two distinct phases is defined by its second-order derivative as the following:[11]

$$\left(\frac{\partial^2 \Delta G_l}{\partial X^2_{\mathrm{Ge}}}\right)_{T,P} = 0 \qquad (2)$$

The necessary condition for a supersaturated melt to be stable is that its second-order derivative is less than zero. At neutral stability, the second-order term vanishes to zero. To determine the point of neutral stability, let us consider the change in free energy of solution. From the Gibbs−Duhem relationship, the

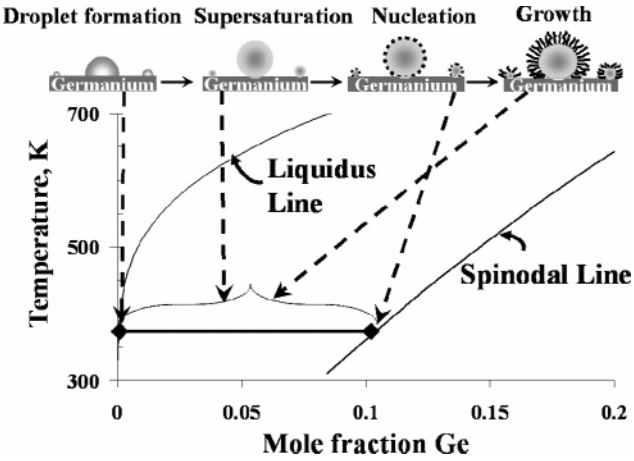


**Figure 5.** Plot showing the liquidus line and the spinodal line for Ge−Ga binary system obtained using the regular solution model, using interaction parameter, Ω, of 16.7 kJ/mol.[5] The proposed nanowire nucleation and growth mechanism involves (a) formation of Ga droplets on Ge substrate, (b) supersaturation of the Ga droplets, (c) spontaneous nucleation of Ge on Ga at the point of instability, and (d) growth of the Ge nuclei in 1-D at composition between the liquidus and spinodal lines.

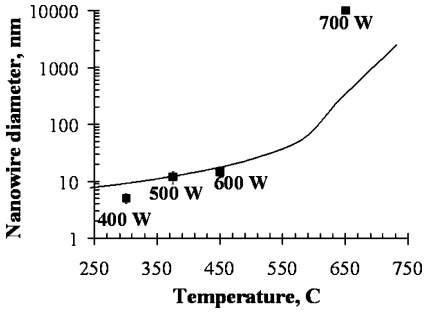


**Figure 6.** The diameter of the nucleus is plotted as a function of synthesis temperature. The solid line represents the diameter predicted by the model. The discrete squares represent the experimentally observed average nanowire diameter at 400, 500, 600, and 700 W incident microwave power with all other reactor parameters being identical to that described in Figure 3.

change in free energy of the solution can be written as

$$\Delta G_l = X_{\mathrm{Ge}} d\mu_{\mathrm{Ge}} + (1 - X_{\mathrm{Ge}}) d\mu_{\mathrm{Ga}} \quad (3)$$

where $X_{\mathrm{Ge}}$ is the mole fraction of Ge, and $\mu_{\mathrm{Ge}}$ and $\mu_{\mathrm{Ga}}$ represent the chemical potentials of Ge and Ga, respectively. After expanding the chemical potential terms on the basis of regular solution model and defining an interaction parameter, Ω, the Gibbs energy change for solution as a function of $T$ and $X_{\mathrm{Ge}}$ is the following:

$$\Delta G_l = RT(X_{\mathrm{Ge}} \ln X_{\mathrm{Ge}} + (1 - X_{\mathrm{Ge}}) \ln(1 - X_{\mathrm{Ge}})) + \Omega X_{\mathrm{Ge}}(1 - X_{\mathrm{Ge}}) \quad (4)$$

The interaction parameter, Ω, is determined to be 16.7 kJ/mol, assuming that the critical temperature is at $X = 0.5$. The composition, $X_{\mathrm{Ge}}$, at which the solution tends to spontaneously decompose into two phases (solid and liquid phases) at a constant temperature, $T$, is determined by solving eqs 3 and 5 simultaneously. In this manner, the loci of points in $T$ and $X$ at which the second differential is zero are determined to describe the spinodal composition line of solute (Si or Ge) in solvent (Ga or In) binary systems. The equilibrium phase diagram and the spinodal curve for Ge−Ga binary system are shown in Figure 5. The point of neutral stability or the spinodal limit is assumed to be the supersaturation at which spontaneous

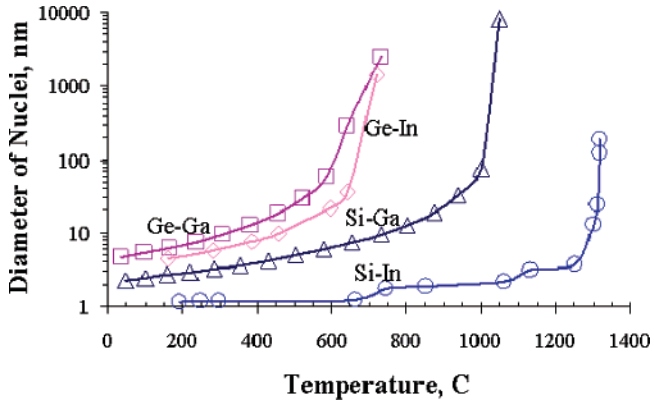


**Figure 7.** The estimated critical nuclei diameter using the solubility limit from the spinodal model is plotted as a function of temperature for Ge−Ga, Ge−In, Si−Ga, and Si−In binary systems. The model predicts that the diameter of the resulting nanowires is different for different molten metal solvents under identical synthesis temperatures.

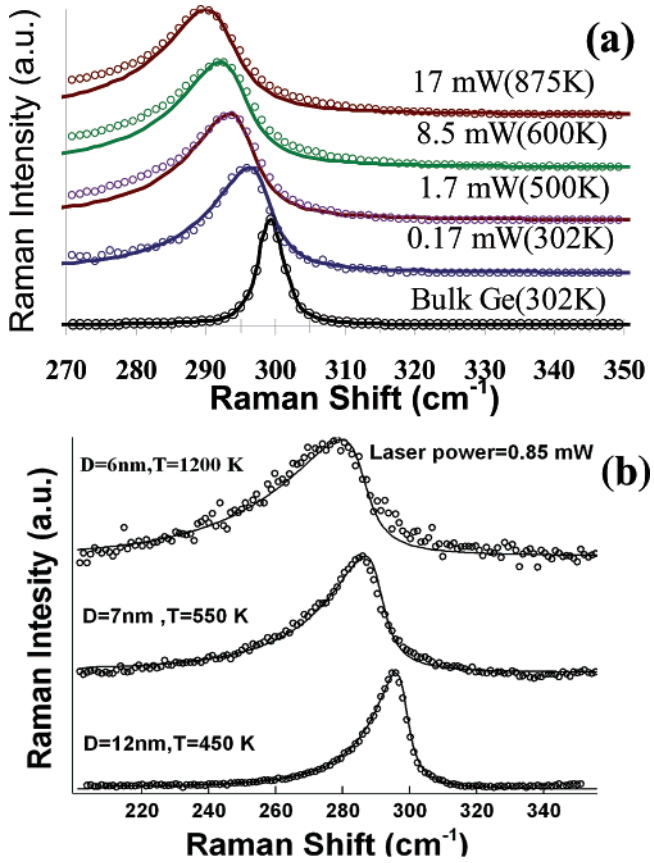


**Figure 8.** (a) Plot showing the first-order Raman peak of Ge nanowires (diameter ~12 nm) at various laser powers. Dotted data points are the phonon confinement line shapes for nanowires with diameter of 12 nm using longitudinal optical phonon dispersion of bulk Ge, temperature, and strain effects; (b) the Raman spectra for nanowire ensembles obtained in different experiments conducted at different synthesis temperatures.

nucleation of the solute from within the low-melting melts occurs. The following equation based on the energy minimization of nuclei formation could be used for estimating the nucleus size (or the resulting nanowire diameter):

$$d_c = \frac{4\underline{V}_M \sigma}{RT \ln\left(\frac{X_{\mathrm{Ge}}}{X_{\mathrm{Ge}}^{\,l}}\right)} \quad (5)$$

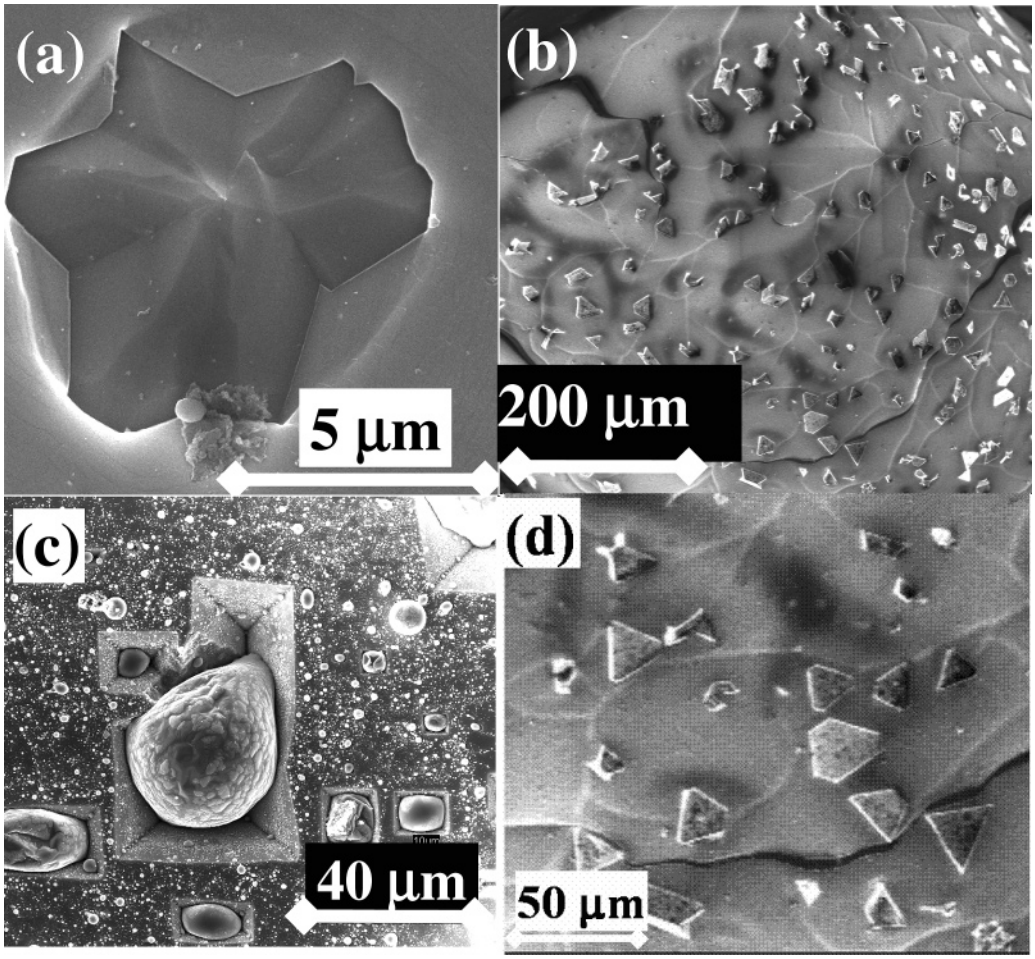


**Figure 9.** (a) and (b) The SEM micrographs showing 2-D and 3-D Ge crystals grown on Ga droplets synthesized using 800 W microwave power and 30 Torr pressure for 1 h using 10 sccm of $H_2$ diluted in 100 sccm of $N_2$; (c) SEM micrographs showing the formation of deep etch pits on the ⟨100⟩ single-crystal Ge substrate at the experimental conditions used in a.



where $d_c$ is the diameter of the resulting nanowire, $\underline{V}_M$ is the molar volume, $\sigma$ is the interfacial energy, and $X_{Ge}/X_{Ge}^{l}$ is the ratio of solute concentration at the point of instability to the corresponding equilibrium solubility at a given temperature, $T$. The schematic of the proposed nucleation and growth mechanism is fully illustrated in Figure 5. As shown in Figure 5, after the nucleation, further growth could occur at solute supersaturation levels below the spinodal limit at any given temperature. Subsequent dissolution into Ga melt beyond nucleation stage sets up a solute concentration supersaturation level that is well below the instability limit for yielding the necessary steady growth rate on the basis of the dissolution rate at steady state. The experiments conducted with increasing growth durations yielded nanowires with increased lengths suggesting that the continuous growth of nanowires is possible and that the growth of nanowires is not self-limiting.

The interfacial energy between the Ga droplet and the Ge substrate is determined to be 2.14 J/m$^2$ using a set of in-situ contact angle measurements, assuming that the surface energy of Ge in a vacuum is 1.76 J/m$^2$.[12] The nucleus diameter predicted by the model is in good agreement with that observed in synthesis experiments as shown in Figure 6. The nucleus size is estimated as a function of temperature and is shown in Figure 7 for both Si and Ge solutes from both gallium and indium melts. Figure 7 indicates that the nanowire diameters could be different for different low-melting metal solvents used at any given synthesis temperature. As an example, the Si nanowire diameter using Ga as solvent could be an order of magnitude larger than that using In as solvent at any synthesis temperature between 500 and 700 °C. In the current study, the microwave plasma used to generate activated hydrogen and chlorine also serves as the heating source for the metal melt solution. The heating of the metal melt occurs through radical recombination of activated gas species at the metal surface. Since the recombination efficiency of the vapor-phase species varies with the type of metals, different metals at the same plasma conditions reach different temperatures which are extremely difficult to measure. So, these particular theoretical predictions have not been confirmed experimentally yet.

Three sets of Ge nanowire growth experiments were performed at varying microwave powers of 400, 500, and 600 W to vary the synthesis temperature between ∼300 and 450 °C. The experiments using chemical vapor transport of Ge onto Ga at temperatures lower than 500 W ($T$ < 350 °C) resulted in sub-10-nm-sized Ge nanowires about one micrometer in length consistently; see SEM photographs in Figure 3b. In our experimental setup, the substrate temperature increases linearly with the incident microwave power. So, in our SLS experiments, the growth rates were found to increase with increasing microwave power or with the substrate temperature used. Higher synthesis temperatures resulted in thicker nanowires as shown in Figure 8a. It turns out that the growth direction of the resulting nanowires changes from [211] to [100] with the increasing synthesis temperature or the faster growth rate or the thickness of the resulting nanowire. These results are described in detail elsewhere.[13] These results are consistent with those obtained

using catalyst clusters under epitaxy with underlying single-crystal substrates that the faster growing Si wires had a growth direction of ⟨110⟩.[14] However, our results here point that the diameters of the growing nanowires do not influence the resulting growth direction.

Micro-Raman spectroscopy of the nanowires could provide an independent confirmation on the average size of nanowires and the size distribution. Previous studies using Raman scattering measurements on Si and Ge nanowires showed the downshifting and asymmetric broadening of the Raman-active optic modes relative to their bulk counterparts because of phonon confinement.[15,16] A detailed modeling considering the contributions from stress, laser-induced heating, and phonon confinement because of nanowire diameter is performed to model the resulting Raman spectra from our nanowire samples. The details of the model are published elsewhere.[17]

The Raman spectra of Ge nanowires at various laser powers are shown in Figure 8a. It can be inferred that as the laser power incident on the nanowire ensemble increases the phonon band downshifts further with enhancing asymmetry. Curve fitting data for lower-laser-induced heating (solid line) are in good agreement with the experimental data (circles) as shown in Figure 8a. Using the model that accounts for both laser-induced heating effects and the phonon confinement model, we then determined the diameter of the nanowire ensemble resulting from the four sets of Ge nanowire samples synthesized at different temperatures. The predicted sizes for nanowires determined using the Raman spectra in Figure 8a agree closely with the theoretically predicted diameters for the corresponding synthesis temperatures using Figure 7. Figure 8b also reveals that as the synthesis temperature is increased the resulting phonon resonance occurs closer to the bulk Ge indicating that the size of the resulting nanowires is higher.

Experiments performed at microwave plasma powers in the range of 700−800 W result in nanowires with diameters between 30 and 100 nm in size. Further experiments using Ga droplets on Ge substrate at microwave plasma powers of 800−1000 W (700−800 °C) resulted in 2-D and 3-D crystals instead of nanowires as shown in Figure 9a and b. At higher synthesis temperatures ($T$ > 700 °C), the estimated nuclei diameter is on the order of micrometers because of expected, low supersaturation limit (Figure 7). In addition, the higher surface diffusion of Ge on Ga and reduced interfacial tension at higher temperatures[8] could induce partial wetting of Ga on Ge substrates. This is experimentally verified through the experimental observation of the irregular shape of Ga droplet on Ge substrates in these experiments at higher temperatures. So, at higher temperatures, the partial wetting and the much reduced supersaturation could have favored the growth of nuclei to grow in 2-D and 3-D versus 1-D.

At low enough synthesis temperatures depending upon the system used, that is, Ga−Si or Ga−Ge, one can obtain high densities of sub-10-nm-sized nanowires using micrometer-sized low-melting metal melt droplets. This is of great advantage toward commercial production of monodispersed, sub-10-nm nanowires for exploiting the quantum confinement based effects of these materials.

## Conclusions

The spinodal decomposition of concentration supersaturated low-melting metal melts explains the observed spontaneous nucleation and growth of high densities of nanowires from larger-sized low-melting metal droplets. The model suggests that the nuclei size decreases with synthesis temperature. The nucleation and growth kinetics of Ge nanowires from a variety of low-melting metal melts are used to validate the proposed nucleation model predictions. Specifically, the size of the resulting Ge nanowires is varied from 4 to 20 nm by increasing the synthesis temperatures approximately from 250 to 500 °C. Uniform diameter distributions were observed for Ge nanowires grown from individual Ga droplets of sizes from 50 nm to 1 mm. The process conditions such as the gas-phase composition including the presence of hydrogen or halogens and gas-phase dissociation (using plasmas) in addition to synthesis temperature determine whether the growth of the nuclei occurs in 1-D or 3-D. At higher synthesis temperatures ($T$ > 600 °C), the Ge crystals grew into 2-D or 3-D morphologies. The model also predicts that the diameter of the resulting nanowires can be different depending upon the low-melting metal melt used.

**Acknowledgment.** We thank Kentucky Science and Technology Corporation (KSTC) and Kentucky NASA-EPSCoR Program for financial assistance.

**Supporting Information Available:** The supplementary information provides information regarding the theoretical calculation of the nucleation density determined using the model. The supplementary information also includes SEM micrographs depicting nanowire growth from different low-melting metals. This material is available free of charge via the Internet at http://pubs.acs.org.

## References and Notes

(1) (a) Wagner, R. S.; Ellis, W. C. *Appl. Phys. Lett.* **1964**, *4*, 89. (b) Morales, A. M.; Lieber, C. M. *Science* **1998**, *279* (5348), 208. (c) Wu, Y. Y.; Yang, P. D. *Chem. Mater.* **2000**, *12* (3), 605. (d) Kammins, T. I.; Li, X.; Williams, R. S.; Liu, X. *Nano Lett.* **2004**, *4*, 503. (e) Dailey, J. W.; Taraci, J.; Clement, T.; Smith, D. J.; Drucker, J.; Picraux, S. T. *J. Appl. Phys.* **2004**, *96* (12), 7556. (f) Wang, D.; Dai, H. *Angew. Chem., Int. Ed.* **2002**, *41* (24), 4783.

(2) Sunkara, M. K.; Sharma, S.; Miranda, R.; Lian, G.; Dickey, E. C. *Appl. Phys. Lett.* **2001**, *79* (10), 1546.

(3) (a) Sharma, S.; Sunkara, M. K. *Nanotechnology* **2004**, *15* (1), 130. (b) Bhimarasetti, G.; Sunkara, M. K. *J. Phys. Chem. B* **2005**, *109* (34), 16219. (b) Sunkara, M. K.; Sharma, S.; Chandrasekaran, H.; Talbott, M.; Krogman, K.; Bhimarasetti, G. *J. Mater. Chem.* **2004**, *14* (4), 590.

(4) (a) Chandrasekaran, H.; Sunkara, M. K. *MRS Symp. Proc.* **2002**, *693*, 159. (b) Li, H.; Chin, A.; Sunkara, M. K. *Adv. Mater.* **2006**, *18*, 216. (c) Rao, R.; Chandrasekaran, H.; Gubbala, S.; Sunkara, M. K.; Daraio, C.; Jin, S.; Rao, A. M. *J. Electron. Mater.* **2006**, *35* (5), 941. (d) Vaddiraju, S.; Mohite, A.; Chin, A.; Meyyappan, M.; Sumanasekera, G.; Alphenaar, B. W.; Sunkara, M. K. *Nano Lett.* **2005**, *5* (8), 1625.

(5) (a) Zheng, B.; Wu, Y.; Yang, P.; Liu, J. *Adv. Mater.* **2002**, *14* (2), 122. (b) Pan, Z. W.; Dai, Z. R.; Ma, C.; Wang, Z. L. *J. Am. Chem. Soc.* **2002**, *124* (8), 1817. (c) Dang, H. Y.; Wang, J.; Fan, S. S. *Nanotechnology* **2003**, *14* (7), 738. (d)Ye, C. H.; Zhang, L. D.; Fang, X. S.; Wang, Y. H.; Yan, P.; Zhao, J. W. *Adv. Mater.* **2004**, *16* (12), 1019. (e) Cai, X. M.; Djurišić, A. B.; Xie, M. H. *J. Appl. Phys.* **2005**, *98*, 074313. (f) Yazdanpanah, M. M.; Haifenist, S.; Safir, A.; Cohn, R. W. *J. Appl. Phys.* **2005**, *98* (7), 073510.

(6) Thurmond, C. D.; Kowalchik, M. *Bell Syst. Technol. J.* **1960**, *39*, 169.

(7) Lu, X.; Fanfair, D.; Johnston, K. P.; Korgel, B. A. *J. Am. Chem. Soc.* **2005**, *127* (45), 15718.

(8) Zaitseva, N.; Harper, J.; Gerion, D.; Saw, C. *Appl. Phys. Lett.* **2005**, *86* (5), 053105.

(9) Nguyen, P.; Ng, H. T.; Meyyappan, M. *Adv. Mater.* **2005**, *17* (5), 549.

(10) Oxtoby, D. W. *J. Phys.: Condens. Matter* **1992**, *4*, 7627.

(11) (a) Cahn, J. W.; Hillard, J. E. *J. Chem. Phys.* **1958**, *28* (2), 258. (b) Cahn, J. W. *J. Chem. Phys.* **1959**, *30* (5), 1121. (c) Cahn, J. W.; Hillard, J. E. *J. Chem. Phys.* **1959**, *31* (3) 688.

(12) Jaccodine, R. J. *J. Electrochem. Soc.* **1963**, *110* (6), 524.

(13) Chandrasekaran, H. Rationalizing Nucleation and Growth in the Vapor-Liquid−Solid (VLS) Method. Ph.D. Dissertation, University of Louisville, 2006.

(14) Schmidt, V.; Senz, S.; Gosele, U. *Nano Lett.* **2005**, *5* (5), 931.

(15) (a) Richter, H.; Wang, Z. P.; Ley, L. *Solid State Commun.* **1981**, *39* (5), 625. (b) Campbell, I. H.; Fauchet, P. M. *Solid State Commun.***1986**,

*58* (10), 739. (c) Adu, K. W.; Gutierrez, H. R.; Kim, U. J.; Sumanasekera, G. U.; Eklund, P. C. *Nano Lett.* **2005**, *5* (3), 409.

(16) (a) Bottani, C. E.; Mantini, C.; Milani, P.; Manfredini, M.; Stella, A.; Tognini, P.; Cheyssac, P.; Kofman, R. *Appl. Phys. Lett.* **1996**, *69* (16), 2409. (b) Zhang, Y. F.; Tang, Y. H.; Wang, N.; Lee, C. S.; Bello, I.; Lee, S. T. *Phys. Rev. B* **2000**, *61* (7), 4518.

(17) Jalilian, R.; Sumanasekera, G. U.; Chandrasekaran, H.; Sunkara, M. K. *Phys. Rev. B* **2006** (in revision).